NeuroImage: Clinical 31 (2021) 102755

Contents lists available at ScienceDirect

NeuroImage: Clinical

journal homepage: www.elsevier.com/locate/ynicl

Resting functional connectivity in the semantic appraisal network predicts accuracy of emotion identification

Winson F.Z. Yang [a,b], Gianina Toller [a], Suzanne Shdo [a], Sonja A. Kotz [b], Jesse Brown [a], William W. Seeley [a], Joel H. Kramer [a], Bruce L. Miller [a], Katherine P. Rankin [a,*]

[a] Memory and Aging Center, Department of Neurology, University of California San Francisco, 675 Nelson Rising Lane, Suite 190, San Francisco, CA 94158, United States

[b] Faculty of Psychology and Neuroscience, Maastricht University, Universiteitssingel 40, 6229 ER Maastricht, Netherlands

ARTICLE INFO

Keywords:
Emotion reading
Functional connectivity
Semantic appraisal network
Right anterior temporal lobe
Neurodegeneration
Frontotemporal dementia

ABSTRACT

Objective: Structural and task-based functional studies associate emotion reading with frontotemporal brain networks, though it remains unclear whether functional connectivity (FC) alone predicts emotion reading ability. The predominantly frontotemporal salience and semantic appraisal (SAN) networks are selectively impacted in neurodegenerative disease syndromes like behavioral-variant frontotemporal dementia (bvFTD) and semantic-variant primary progressive aphasia (svPPA). Accurate emotion identification diminishes in some of these patients, but studies investigating the source of this symptom in patients have predominantly examined structural rather than functional brain changes. Thus, we investigated the impact of altered connectivity on their emotion reading.

Methods: One-hundred-eighty-five participants (26 bvFTD, 21 svPPA, 24 non-fluent variant PPA, 24 progressive supranuclear palsy, 49 Alzheimer's disease, 41 neurologically healthy older controls) underwent task-free fMRI, and completed the Emotion Evaluation subtest of The Awareness of Social Inference Test (TASIT-EET), watching videos and selecting labels for actors' emotions.

Results: As expected, patients averaged significantly worse on emotion reading, but with wide inter-individual variability. Across all groups, lower mean FC in the SAN, but not other ICNs, predicted worse TASIT-EET performance. Node-pair analysis revealed that emotion identification was predicted by FC between 1) right anterior temporal lobe (RaTL) and right anterior orbitofrontal (OFC), 2) RaTL and right posterior OFC, and 3) left basolateral amygdala and left posterior OFC.

Conclusion: Emotion reading test performance predicts FC in specific SAN regions mediating socioemotional semantics, personalized evaluations, and salience-driven attention, highlighting the value of emotion testing in clinical and research settings to index neural circuit dysfunction in patients with neurodegeneration and other neurologic disorders.

1. Introduction

Emotion reading requires multiple social cognitive processes, including the ability to attend to, perceive, and identify another's emotion, as well as to label and make inferences about the meaning of the emotion (Mitchell, 2009). It is important for successful development and maintenance of communication in interpersonal relationships. Poor emotion reading skills are frequently reported in patients with neurodegenerative (NDG) syndromes such as behavioral-variant frontotemporal dementia (bvFTD), semantic variant primary progressive aphasia (svPPA) and Alzheimer's disease syndrome (ADs) (Hutchings et al., 2017). Investigations of the neural correlates of emotion reading in these patients have typically used structural region-of-interest (ROI) or voxel-based morphometry approaches (Baez et al., 2016; Kumfor et al., 2018), or task-based functional magnetic resonance imaging (fMRI) studies (Marshall et al., 2019) rather than examining network

* Corresponding author.
E-mail addresses: winson.yang@alumni.maastrichtuniversity.nl (W.F.Z. Yang), Gianina.Toller@ucsf.edu (G. Toller), Suzanne.Shdo@ucsf.edu (S. Shdo), sonja.kotz@maastrichtuniversity.nl (S.A. Kotz), Jesse.Brown@ucsf.edu (J. Brown), Bill.Seeley@ucsf.edu (W.W. Seeley), joel.kramer@ucsf.edu (J.H. Kramer), Bruce.Miller@ucsf.edu (B.L. Miller), Kate.Rankin@ucsf.edu (K.P. Rankin).

https://doi.org/10.1016/j.nicl.2021.102755
Received 29 March 2021; Received in revised form 1 July 2021; Accepted 3 July 2021
Available online 7 July 2021

connectivity as a trait (Rankin, 2020). Work in the last decade has highlighted the selective vulnerability of specific intrinsically connected networks (ICNs) in these NDG syndromes (Seeley et al., 2009), but has primarily centered on disease-related changes to these ICNs (Zhou et al., 2010), with few directly investigating how altered ICN function may cause characteristic behavioral symptoms like emotion reading impairments (Marshall et al., 2019; Van den Stock et al., 2017).

ICNs are normally-occurring functional networks (Dosenbach et al., 2007) that underlie specific cognitive, motor, and behavioral functions (Laird et al., 2011; Nickerson, 2018; Smith et al., 2009). Two ICNs that are focally impacted in NDG syndromes in which patients evidence disrupted socioemotional behavior (Rankin, 2020), are the salience network (SN), affected in bvFTD, and the semantic appraisal network (SAN), affected in both svPPA and some bvFTD patients (Ranasinghe et al., 2016b; Seeley et al., 2009). The SN has key hubs in the ventral anterior insula (AI) and the dorsal anterior cingulate cortex (dACC) (Seeley et al., 2007a). It identifies stimuli with personal salience, integrates sensory, visceral, and autonomic signals, filters information to focus attention on stimuli that are homeostatically relevant for an individual, and provides visceral motivation for a response (Seeley, 2019). The pivotal role of the SN in socioemotional symptoms in bvFTD is well-established (Rijpma et al., 2021; Seeley et al., 2012; Toller et al., 2018).

Mapping of the variously named "limbic" network or SAN as a functionally distinct intrinsic network has been performed in multiple studies of healthy individuals (Buckner et al., 2011; Choi et al., 2012; Yeo et al., 2014, 2011). The SAN has a key hub in the anterior temporal lobe (aTL), and also includes rostromedial prefrontal cortex (rostromedial PFC), subgenual anterior cingulate cortex (subgenual ACC), nucleus accumbens, and basolateral amygdala (basolateral amygdala). These SAN nodes are involved in storage and retrieval of multimodal semantic information (Patterson et al., 2007) as well as providing a personalized appraisal of semantic information, tagging entities with complex hedonic evaluations (Seeley et al., 2012; Stein et al., 2007). According to the controlled semantic cognition theory (Binney and Ramsey, 2020; Lambon Ralph et al., 2017), semantic processing of both non-social and socioemotional information requires multimodal inputs from multiple brain regions and networks ("spokes"), but the aTL is the semantic "hub" where these inputs converge. Clinical evidence has also revealed that patients with degeneration of the aTL SAN hub exhibit disruption of semantic representation (Guo et al., 2013; Hodges and Patterson, 2007; Seeley et al., 2012), including for social (Pobric et al., 2016) and emotional concepts (Olson et al., 2013; Rankin, 2020). The right anterior temporal lobe (RaTL) and orbitofrontal evaluation regions are bidirectionally anatomically connected via the uncinate fasciculus white matter tract (Ghashghaei and Barbas, 2002), and have previously been identified as important for facilitating the emotion identification process (Olson et al., 2013). Stronger structural connectivity between the RaTL and subgenual ACC nodes of the SAN via the uncinate fasciculus has also been associated with better emotion reading abilities (Multani et al., 2017; Papinutto et al., 2016). The RaTL receives more sensory input relevant to emotional experience than the LaTL does (Rice et al., 2015), and thus may be comparatively more active in processing emotional semantics. The relationship between trait-level "resting" connectivity in ICNs and functional activation patterns during tasks is still being defined (Multani et al., 2017; Nickerson, 2018; Papinutto et al., 2016; Smith et al., 2009); however, numerous studies have related trait-level resting ICN connectivity with individuals' cognitive abilities and characteristics (Battistella et al., 2019; Seeley et al., 2007b; Toller et al., 2018, 2019).

The primary aim of this study was to investigate whether accuracy on an emotion identification task would be predicted by SAN and SN functional connectivity, examining the contribution of both mean network connectivity and connectivity among cortical and subcortical ICN node pairs. Our goal was to provide evidence supporting the existence of this brain-behavior relationship, and we chose to study a diverse group of neurodegenerative disease patients because, unlike healthy controls, individual patients have variable degrees of impairment in emotion reading, as well as disconnection of these key ICNs, providing broad enough variance for linear modeling of this brain-behavior relationship. While we expected to replicate the many previous studies showing that in early stages, bvFTD and svPPA patient groups would perform worse than controls on an emotion identification task, reiterating this well-established finding or otherwise characterizing the broader socioemotional functioning of these patients was not central to this study.

We designed the study to show the specificity of this brain-behavior relationship, hypothesizing that better emotion identification would be related to higher mean connectivity in the SAN and the SN, but not to connectivity in two "control" networks, the default-mode network (DMN) and the sensorimotor network (SMN). While the SMN was chosen because it is not directly involved in socioemotional processing and thus is a true "nonsocial control network", we also chose the DMN as a "social control network" to further challenge the specificity of the hypothesized relationship between emotion reading and SAN and SN connectivity. The DMN mediates some aspects of social functioning, including theory of mind and self-referential contextualization (Rankin, 2020), and plays a role in semantic processing (Binder et al., 2009). The DMN does include an anterior temporal node, though this is more weakly correlated with other DMN nodes such as the inferior parietal lobule (Andrews-Hanna et al., 2010). While these anterior temporal contributions to DMN functioning suggest this network may utilize semantic knowledge, given the distinctly memory-related core functions of the DMN, we hypothesized that mean connectivity in the DMN would not directly contribute to variability in emotion reading accuracy (Andrews-Hanna et al., 2010; Buckner and DiNicola, 2019; Humphreys et al., 2015; Wang et al., 2019).

Furthermore, because this is the first study to examine how functional connectivity in these networks relates to emotion reading, we chose to make a secondary analysis exploring the relationship of emotion reading to all node pairs in any ICN for which overall mean connectivity was a significant predictor. Based on the established importance of the ATL in both socioemotional and non-social semantic processing, we predicted that connectivity between the rATL and other cortical and subcortical structures of the SAN, and particularly the subgenual ACC and rostromedial PFC regions of the orbitofrontal cortex (OFC), would play a particularly notable role in emotion reading in this secondary node pair analysis.

2. Methods

2.1. Participants

A total of 185 individuals, including 144 patients in very early stages of five different NDG syndromes and 41 healthy older controls (HC) were recruited from the University of California San Francisco Memory and Aging Center. Of the 144 individuals with NDG, 26 were diagnosed with bvFTD (Rascovsky et al., 2011), 49 with AD syndrome (McKhann et al., 2011), 21 with svPPA (Gorno-Tempini et al., 2011), 24 with nonfluent variant primary progressive aphasia (nfvPPA) (Gorno-Tempini et al., 2011), and 24 with progressive supranuclear palsy (PSP) (see Table 1) (Litvan et al., 1996). Clinical diagnoses were determined by a consensus team of neurologists, neuropsychologists, and nurses through a review of thorough neurological, structural neuroimaging, and neuropsychological assessments. Inclusion criteria for the patient groups were Clinical Dementia Rating (CDR) score $\leq$1 (i.e., mild to very mild neurocognitive disorder), and valid TASIT-EET obtained within 90 days of neuroimaging. Inclusion criteria for the HC group included an unremarkable neurological and structural MRI exam, and no functional or cognitive deficits based on thorough history and neuropsychological evaluation. The study was approved by the UCSF Committee on Human Research and participants gave informed consent.

Table 1
Demographics and clinical characteristics of the sample (n = 185).

Mean (SD)	HC (n = 41)	AD (n = 49)	bvFTD (n = 26)	nfvPPA (n = 24)	PSP (n = 24)	svPPA (n = 21)	F-statistic	p-value
Age	68.71 (7.06)	61.18 (7.50)***	60.08 (8.95)***	67.08 (8.52)	67.54 (7.40)	64.05 (6.31)	7.37	<0.001
Sex (M/F)	12/29	21/30	16/10	9/15	12/12	10/11	$\chi^2 = 7.74$	n.s.
Education	17.51 (2.24)	16.65 (2.77)	16.69 (4.05)	16.67 (3.68)	15.67 (3.99)	17.76 (3.25)	1.38	n.s.
MMSE	29.27 (0.84)	22.86 (3.30)***	26.23 (2.47)***	26.21 (2.65)***	25.58 (3.56)***	25.48 (2.84)***	24.32	<0.001
CDR	0.00 (0.00)	0.68 (0.28)***	0.83 (0.24)***	0.38 (0.30)***	0.75 (0.26)***	0.62 (0.27)***	57.93	<0.001
EXECUTIVE								
Digit span forward [a]	7.06 (1.10)	4.78 (0.98)***	5.75 (1.26)***	4.70 (1.02)***	5.17 (0.89)***	6.81 (1.44)	27.66	<0.001
Digit span backwards [a]	5.50 (1.44)	3.06 (0.85)***	3.79 (1.44)***	3.57 (0.99)***	3.61 (1.16)***	4.90 (1.37)	20.57	<0.001
Modified Trails (lines/min) [a]	41.25 (17.25)	8.41 (9.19)***	19.79 (13.40)***	17.75 (9.10)***	13.86 (11.08)***	22.90 (11.96)***	29.14	<0.001
LANGUAGE								
BNT [a]	14.56 (0.81)	11.36 (3.33)***	13.64 (1.59)	12.54 (2.41)*	13.50 (1.77)	5.45 (3.85)***	39.79	<0.001
VISUOSPATIAL								
VOSP number location [a]	9.22 (1.31)	6.18 (2.93)***	8.57 (1.24)	8.92 (1.18)	8.18 (1.76)	9.40 (1.10)	14.75	<0.001
Benson Figure Copy[a]	15.36 (0.95)	11.24 (5.80)***	15.21 (0.83)	15.30 (0.97)	13.00 (2.60)	15.48 (1.17)	8.85	0.018
CATS-FM[a]	11.80 (0.58)	10.77 (1.68)*	10.54 (1.74)*	11.23 (1.63)	10.47 (1.90)***	11.90 (0.30)	4.05	0.0064
MEMORY								
CVLT-SF (30 s delay)[a]	9.00 (0.00)	3.74 (2.21)***	5.48 (2.43)*	6.57 (1.75)	6.04 (1.97)	3.35 (2.81)***	10.58	<0.001
CVLT-SF (10 min delay)[a]	9.00 (0.00)	2.74 (2.64)***	4.35 (2.85)**	6.17 (2.08)	5.61 (2.21)	2.05 (2.33)***	13.17	<0.001
Benson Figure 10 min Delay[a]	9.97 (0.85)	4.19 (0.75)***	5.38 (0.90)***	9.78 (0.92)	5.80 (0.92)***	7.73 (0.97)*	13.60	<0.001
TASIT-EET[a]	10.53 (0.38)	9.51 (0.34)***	8.51 (0.41)***	9.46 (0.41)*	10.06 (0.41)***	7.35 (0.44)***	14.19	<0.001

Dunnett post-hoc tests were used to analyze group differences in age, MMSE, and CDR. Dunnett-Hsu post-hoc tests controlling for age and sex were used to compare neuropsychological tests, least-square mean scores between the patient groups and the control group. n.s. = non-significant, HC = Healthy Control, AD = Alzheimer's disease, bvFTD = behavioral variant frontotemporal dementia, nfvPPA = nonfluent variant primary progressive aphasia, PSP = progressive supranuclear palsy, svPPA = semantic variant primary progressive aphasia, MMSE = Mini-Mental State Examination, CDR = Clinical Dementia Rating, CVLT-SF = California Verbal Learning Test Short Form, BNT = Boston Naming Task, VOSP = Visual Object and Space Perception Battery, BFC = Benson Figure Copy, BFR = Benson Figure Recognition, CATS-FM = Comprehensive Affect Testing System-Face Matching, TASIT-EET = The Awareness of Social Interference Test, Emotion Evaluation Task.
[a] Dunnett-Hsu post-hoc comparisons of least-square means against healthy controls were adjusted for age and sex.
* $p < 0.05$,
** $p < 0.01$,
*** $p < 0.001$.

2.2. Behavioral measures

2.2.1. The Awareness of Social Inference Test, Emotion Evaluation Test

After diagnosis and enrollment, patients underwent emotion testing as part of a larger battery of social and general neuropsychological cognition tests. An abbreviated form of The Awareness of Social Inference Test, Emotion Evaluation Test (TASIT-EET) (McDonald et al., 2004) was used to measure participants' ability to identify the six basic emotions (happy, sad, disgusted, surprised, angry, frightened), using 14 videos (~20 s duration) in which actors expressed emotions through facial, vocal, and gestural modalities. The scripts are neutral in spoken semantic content, but the actors express the emotion using matched facial, vocal prosody, and gestural cues. After each video, participants are asked to select the correct emotion label from six options. Neuropsychological testers had significant experience evaluating dementia patients, and were instructed to discontinue testing if there was evidence of test invalidity, i.e. if patients showed difficulty comprehending the verbal emotion labels or were otherwise not able to comply with test procedures. Therefore, some patients with severe language comprehension deficits likely did not receive the TASIT-EET and were excluded from this sample.

2.2.2. Neuropsychological assessment

In order to provide a more comprehensive depiction of the patients' cognitive characteristics apart from emotion reading, data was obtained from the original diagnostic neuropsychological evaluation. This battery of tests has been described comprehensively elsewhere (Ranasinghe et al., 2016b); briefly, tests of memory, executive functioning/attention, visuospatial functioning, and language were included, and are listed in Table 1. Particularly relevant to analyses for this study, the 10-minute delayed free recall of the Benson Complex Figure (BFD) (Possin et al., 2011) was administered to assess participants' nonverbal episodic memory performance. This non-social task was used to validate the brain-behavior specificity of our findings through a double dissociation, expecting that the BFD memory score would correlate with mean connectivity in the memory network (i.e. the DMN) but not with the SAN, SN, or SMN.

2.3. Resting-state functional imaging

2.3.1. Image acquisition

Participants underwent functional and structural neuroimaging using a 3T Siemens Trio scanner with 8 min eyes closed FC magnetic resonance imaging (fcMRI) protocol. Functional and structural images were obtained using a 3T Siemens Trio scanner using a standard 12-channel head coil. A volumetric magnetization prepared rapid gradient echo (MPRAGE) sequence was used to acquire T1-weighted images of the entire brain, with parameters as follows: 160 sagittal slices, 1-mm thick, skip = 0 mm; repetition time = 2300 ms; echo time = 2.98 ms; flip angle = 9°; field of view = 240 × 256 mm^2; voxel size = 1 mm^3; matrix size = 256 × 256. Two hundred and forty task-free functional images were obtained using an 8-minute T2*-weighted echo planar imaging sequence (36 axial slices, 3-mm thick, slice-gap = 0.6 mm, repetition time = 2000 ms; echo time = 27 ms; accel = 2; flip angle = 80°; field of view = 230 × 230 mm^2; inplane voxel size = 2.5 mm^2; matrix size = 92 × 92). The sequence was acquired with an online gradient adjustment to compensate for head motion.

2.3.2. Image preprocessing and analysis

The images were preprocessed and analyzed using Statistical Parametric Mapping 12 (SPM; https://www.fil.ion.ucl.ac.uk/spm) running on MATLAB 2015a (Ashburner et al., 2020) and the FMRIB Software Library (FSL; http://www.fmrib.ox.ac.uk/fsl/). The first five volumes were discarded to allow for magnetic field stabilization. Images were then slice-time corrected, spatially realigned, co-registered to each participant's structural T1-weighted image, and normalized to the

Montreal Neurological Institute (MNI) template. The images were re-sampled at a voxel size of 2 mm^3, and smoothed with a 6 mm full-width at half-maximum Gaussian kernel. A band pass filter ranging between 0.0083 and 0.15 was applied to reduce the effect of low frequency drift and high-frequency noise (Lowe et al., 1998).

Structural T1-weigthed images were preprocessed using SPM12. The images were visually inspected for artifacts, bias-corrected, tissue classified (gray matter, white matter, cerebrospinal fluid segments), spatially normalized using SPM12's default low-dimensional spatial normalization step, modulated, and smoothed with a 8-mm FWHM isotropic Gaussian kernel. The resulting smoothed, modulated, segmented, and normalized gray matter images were resampled at a voxel size of 2 mm^2 to match the resolution of the ICN masks described in Section 2.3.4.

2.3.3. Head motion correction

The motion parameters estimated during spatial realignment were used to compute the magnitude of head motion during each scan. This is because head motion can induce systematic but spurious correlations, particularly in older adults and clinical populations (Power et al., 2012). Only participants who fulfilled all the following criteria were included into the study: maximum translational movement $\leq$3 mm, maximum rotational movement $\leq 3^{\circ}$, maximum displacement $\leq$3 mm between functional volumes, and spikes (max displacement >1 mm) occurring in <10% of all 240 volumes. Forty-four participants who were otherwise eligible and had complete data did not meet these movement criteria and were excluded from the study. Mean root-mean-square of volume-to-volume changes in translational (in mm) and rotational (mean Euler angle) movement were calculated. These values were computed because these metrics can be associated with intrinsically connected network (ICN) strength (Van Dijk et al., 2012). A general linear model (GLM) with age, sex, and Mini-mental State Examination (MMSE) as covariates, was computed to examine group differences in head motion parameters. The GLM confirmed that there were no group differences in translational or rotational head movements (Table 2).

2.3.4. Derivation of mean ICN connectivity

To derive values for mean network connectivity in the SAN, SN, and the two "control" networks (DMN and SMN), ROI-based ICN analysis was conducted by selecting the hub region of each network and mapping the distribution of connected regions. The DMN and SMN were included as control networks with the expectation that TASIT-EET score would be predicted by connectivity specifically in the SAN, but not by connectivity in the DMN or SMN, thereby demonstrating the specificity of the hypothesized ICN-behavior relationship. The SMN was chosen as a non-social control network, and the DMN was chosen as a social control network because it has previously been associated with memory and theory of mind (i.e. intention attribution) (Andrews-Hanna et al., 2014; Caminiti et al., 2015; Rijpma et al., 2021) but not with emotion reading. The hub region for deriving each network was selected from published studies (Beissner et al., 2013; Yeo et al., 2011), and mean connectivity was calculated separately for each network (SAN, SN, DMN, SMN) in each participant by computing the mean beta values across all voxels within each ICN-specific mask height and extent thresholded mask ($p_{FWE} < 0.001$). The ROIs used to derive four ICNs are: (1) right anterior temporal pole (RaTP) at Montreal Neurological Institute (MNI) coordinates (36, 22, −34) for the SAN (Yeo et al., 2011), (2) right ventral anterior insula (42, 17, −10) for the SN (Seeley et al., 2007a), (3) posterior cingulate cortex (−8, −56, 26) for the DMN (Andrews-Hanna et al., 2014), and (4) right precentral gyrus (28, −16, 66) for the SMN (Zielinski et al., 2010).

MARSBAR toolbox (Brett et al., 2002b) was used to create spheres of 4 mm radius centered on the MNI coordinates of the chosen ROIs. MARSBAR toolbox was also used to extract the average blood oxygen level-dependent (BOLD) signal time series of all voxels at each of the 235 volumes within each ICN's ROI. The average BOLD signal time series for each ROI was then used as a covariate of interest in a whole-brain regression model to derive the t-map for each ICN for each participant. A cerebrospinal fluid (CSF) mask in the central portion of the lateral ventricles and a white matter (WM) mask based on the highest probability in the (FMRIB Software Library) FSL tissue probability mask were used to extract mean CSF and WM timeseries. These were included as covariates of no interest, along with each participant's 6 motion parameters, their temporal derivatives, and the squares of all previous terms. 32 total covariates of no interest were included in the design matrix.

2.3.5. Atrophy correction

For each participant, the mean number of gray matter voxels was calculated separately within the binary SAN and SN mask, and was used as a confounding covariate 1) in order to better control for pathological changes in gray matter structure coming from our patient samples, and 2) to obtain a more generalizable measure of the relationship of TASIT-EET and BFD, respectively, to mean SAN and SN connectivity, apart from any influence of volume.

2.3.6. Derivation of ICN node-pairs

To investigate which specific patterns of within-network functional connectivity were predictors of TASIT-EET scores, cortical and subcortical ROIs representing the key functional nodes for each network were

Table 2
Motion parameters and mean ICN connectivity of the sample.

Mean (SE)	HC (n = 41)	AD (n = 49)	bvFTD (n = 26)	nfvPPA (n = 24)	PSP (n = 24)	svPPA (n = 21)	F-statistic	p-value
rs-fMRI preprocessing								
translational motion (mRMS), mm	0.87(0.11)	0.85(0.10)	0.95(0.12)	0.83(0.12)	1.09(0.12)	0.67(0.13)	1.34	n.s.
Max rotation (mEuler), degrees	0.77(0.11)	0.63(0.10)	0.76(0.12)	0.60(0.12)	0.79(0.12)	0.90(0.13)	0.83	n.s.
rs-fMRI ICN analysis								
Mean SAN connectivity	0.11(0.0086)	0.06(0.0077)***	0.05(0.0092)***	0.07(0.0094)**	0.07(0.0093)**	0.06(0.0099)***	6.09	<0.001
Mean SN connectivity	0.081(0.0062)	0.071(0.0056)	0.061(0.0066)	0.058(0.0068)*	0.066(0.0067)	0.065(0.0072)	1.86	n.s
Mean DMN connectivity	0.14(0.0075)	0.090(0.0066)***	0.097(0.0079)**	0.11(0.0081)*	0.10(0.0081)*	0.97(0.0086)**	3.91	<0.01
Mean SMN connectivity	0.16(0.010)	0.10(0.009) **	0.09(0.011)***	0.09(0.011)**	0.10(0.011)**	0.11(0.012)*	5.38	<0.001

Motion parameters, and mean ICN connectivity, were controlled for age, sex, and MMSE. Dunnet-Hsu post-hoc tests were used to compare least-square means between each patient group and the control group. n.s. = non-significant, HC = Healthy Control, AD = Alzheimer's disease, bvFTD = behavioral variant frontotemporal dementia, nfvPPA = nonfluent variant primary progressive aphasia, PSP = progressive supranuclear palsy, svPPA = semantic variant primary progressive aphasia, mRMS = mean root-mean-square, mEuler = mean Euler, SAN = semantic appraisal network, SN = salience network, DMN = default mode network, SMN = sensorimotor network.

* $p < 0.05$.

** $p < 0.01$,

*** $p < 0.001$ at group comparisons against the HC group

selected, including bilateral aTP at MNI coordinates (±36, 22, −34), rostromedial PFC (orbital gyrus (±20, 59, −15), anterior gyrus rectus (±4, 58, −20)), subgenual ACC (±4, 20, −15), nucleus accumbens (10, 11, −9), and the basolateral amygdala (±20, −6, −18) (see Fig. 1) (Beissner et al., 2013; Yeo et al., 2011). MARSBAR toolbox for SPM12 (Brett et al., 2002a) was used to create 4 mm spherical ROIs were centered on the peak coordinates of the aTP, orbital gyrus, anterior gyrus rectus, subgenual ACC, and nucleus accumbens. To avoid an overlap of the ROIs centered on the amygdalae, a ROI size of 3 mm was chosen for the basolateral amygdala. Each ROI's mean voxelwise BOLD signal time series was used to calculate correlations with all other node-pairs, controlling for the same 32 CSF, white matter, and motion regressors as described above. To reduce the number of pairwise comparisons, we also created four summary scores to group regional nodes along the anterior-posterior gradient in the orbitofrontal cortex (OFC) (Kringelbach and Rolls, 2004) by summing pairwise connectivity among multiple ROIs: subgenual ACC and nucleus accumbens ROIs were combined as the right (1) and left (2) posterior OFC evaluation node scores. Orbital gyrus and anterior gyrus rectus ROIs were combined as the (3) right and (4) left anterior OFC evaluation node scores.

2.4. Statistical analysis

2.4.1. Behavioral data analyses

After undergoing regression diagnostics, differences on TASIT-EET and BFD scores across diagnostic groups were investigated via general linear modelling using the lm function in R 3.5.2, controlling for age, sex, and MMSE, with Dunnett-Hsu post-hoc testing.

2.4.2. Mean network and node-pair-based connectivity analyses

General linear modelling was performed to determine whether mean network connectivity in any of the four networks predicted TASIT-EET scores, controlling for age, sex, and MMSE. Primary analyses modeled the independent SAN and SN contributions and their interactions, followed by secondary analyses to error check significant models for confounding effects of brain volume (see Toller et al., 2018 for detailed rationale and methods) and diagnostic group (see Rankin et al., 2009; Sollberger et al., 2009). Briefly, diagnostic group was parameterized and included in the model as a nuisance predictor to determine if main effects were disproportionately influenced by a single diagnostic group. Specificity analyses were used to confirm that TASIT-EET was not predicted by DMN or SMN connectivity and that BFD scores were predicted by DMN but not SAN, SN, or SMN connectivity. We then calculated each participant's correlation coefficients between each of the following nodes: (1) right posterior OFC evaluation node, (2) left posterior OFC evaluation node, (3) right anterior OFC evaluation node, (4) left anterior OFC evaluation node, (5) right anterior temporal pole (RaTP), (6) left anterior temporal pole (LaTP), (7) right basolateral amygdala, and (8) left basolateral amygdala. FC was also examined among subsets of eight cortical and subcortical nodes found significant at the mean connectivity level, correcting for k = 28 comparisons using a Benjamini-Yekutieli threshold of $p < 0.01273$. The FC between these nodes were analyzed with separate regressions, each consisting of the covariates (age, sex, MMSE).

3. Results

3.1. Demographics and clinical characteristics

AD and bvFTD patients were significantly younger than HCs, and AD patients had lower MMSE scores than most other patient groups (Table 1). CDR scores among patient groups ranged from 0.5 to 0.8, well within the very mild dementia range, thus statistical differences likely did not reflect meaningful clinical differences in severity among patient groups. No other group differences were found, but all subsequent regression analyses included age, sex, and MMSE as potentially confounding covariates. Neuropsychological characterization of the patient sample on a multi-domain battery of cognitive tests can be found in Table 1.

3.2. Behavioral results

After controlling for age, sex and MMSE, patients with bvFTD (*lsmean* ± *SE*: 8.51 ± 0.41, $p < 0.01$) and svPPA (7.35 ± 0.44, $p < 0.001$) had significantly lower TASIT-EET scores than HCs (10.53 ± 0.38). AD (4.19 ± 0.75), bvFTD (5.38 ± 0.90) and PSP (5.80 ± 0.92) patients

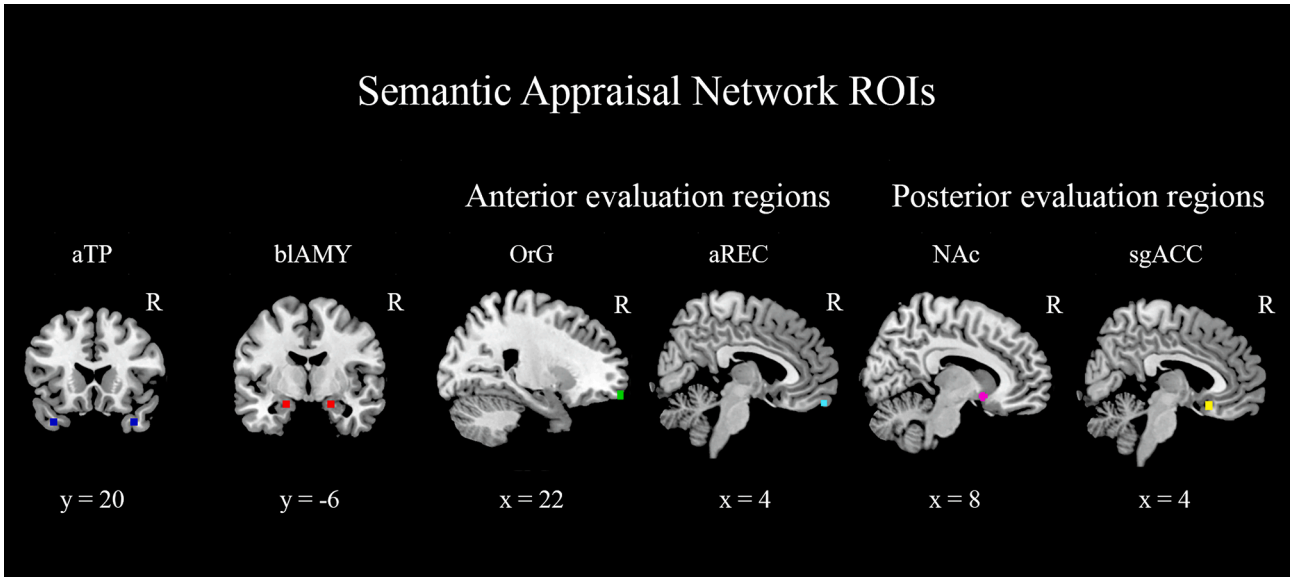

Fig. 1. shows the regions of interest used for the node pair connectivity analyses in the semantic appraisal network. Sagittal slices shown are in the right hemisphere. aTP = anterior temporal pole, blAMY = basolateral amygdala, OrG = orbital gyrus, aREC = anterior gyrus rectus, NAc = nucleus accumbens, sgACC = subgenual anterior cingulate cortex. Blue = aTP [±36, 22, −34], red = blAMY [±20, −6, −18], green = OrG [±20, 59, −15], cyan = aREC [±4, 58, −20], violet = NAc [±10, 11, −9], yellow = sgACC [±4, 20, −15]. Coordinates shown are the Montreal Neurological Institute (MNI) coordinates. (For interpretation of the references to colour in this figure legend, the reader is referred to the web version of this article.)

scored significantly lower on the BFD than HCs (9.97 ± 0.85). Results in Table 1 show these and other neuropsychological test comparisons between patients and controls, controlling for age and sex only because of the shared variance between MMSE and the cognitive tests.

3.3. Neuroimaging results

3.3.1. Mean network connectivity-based ICN analysis

We found that in independent models, higher mean connectivity in the SAN (adjusted r = 0.54, $p < 0.001$) and in the SN ($r_{adj} = 0.27$, $p < 0.05$) predicted higher TASIT-EET scores. When mean SAN and SN connectivity were modelled together, mean connectivity in the SAN still independently predicted TASIT-EET scores controlling for SN ($r_{adj} = 0.54$, $p < 0.01$; Fig. 2), though the SN was no longer a predictor when modelled alongside the SAN, and the SN/SAN interaction was non-significant. This suggests that the initial independent model suggesting that SN was a significant predictor of TASIT-EET was likely due to confounding by the high intra-individual correlation of SAN and SN connectivity (r = 0.46, $p < 0.001$). Higher SAN connectivity still predicted higher TASIT-EET scores after atrophy correction ($r_{adj} = 0.53$, $p < 0.001$) and error checking for confounding effects of diagnostic group membership ($r_{adj} = 0.48$, $p < 0.05$).

Mean connectivity in neither of the two "control" networks, the DMN or the SMN, predicted TASIT-EET scores, supporting the specificity of the TASIT-EET/SAN relationship. The BFD (memory) score was predicted by mean connectivity in the DMN ($r_{adj} = 0.43$, $p < 0.05$), but not by mean connectivity in the SAN, SN, or SMN (all $p > 0.05$), providing evidence that results were due to specific ICN-cognition relationships, rather than due to non-specific brain degeneration and resulting generalized cognitive deficits.

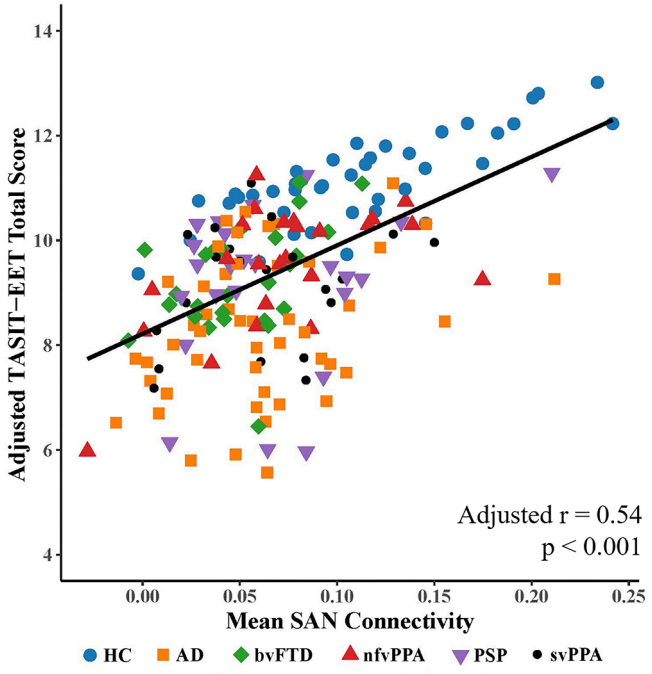

Fig. 2. displays the relationship between mean connectivity in the semantic appraisal network (SAN) and the TASIT-EET in the full sample of healthy older controls and patients with neurodegenerative diseases (n = 185), after adjusting for age, sex, MMSE, and mean salience network connectivity. Mean SAN connectivity significantly predicted TASIT-EET score after adjusting for age, sex, MMSE, and after including the salience network in the model (r = 0.54, p < 0.01). Higher mean SAN connectivity was associated with higher TASIT-EET score. Mean connectivity values were calculated as each participant's mean beta value across all voxels within their given ICN map, masked at the ICN as defined in an independent sample of healthy older participants (see methods). HC = healthy control, AD = Alzheimer's disease, bvFTD = behavioral variant frontotemporal dementia, nfvPPA = nonfluent variant primary progressive aphasia, PSP = progressive supranuclear palsy, svPPA = semantic variant primary progressive aphasia, TASIT-EET = The Emotional Evaluation Task of the Awareness of Social Interference Test.

3.3.2. Node-pair based ICN analysis

Our node-pair based analysis revealed that significant predictors of TASIT-EET total score included FC between: (1) the RaTP and the right posterior OFC evaluation node (r = 0.19, $p = 0.008$), (2) the RaTP and the right anterior OFC evaluation node (r = 0.24, $p = 0.001$), and (3) the left basolateral amygdala and the left posterior OFC evaluation node (r = 0.19, $p = 0.009$). Connectivity between: (4) the RaTP and left posterior OFC evaluation node (r = 0.18, $p = 0.016$), and (5) the left basolateral amygdala and right posterior OFC evaluation node (r = 0.18, $p = 0.014$) showed a trend towards significance that did not survive correction for multiple comparisons (B-Y threshold < 0.01273; Fig. 3). All these relationships remained significant after atrophy correction, and (1) and (2) remained significant after error checking for regional atrophy and diagnostic confounding.

4. Discussion

The primary result from this study was the demonstration that mean functional connectivity in the SAN, i.e., the intrinsically connected network mediating semantic appraisal, was a significant predictor of how accurately patients could identify emotions shown in realistic videos. This association was driven primarily by functional connectivity between the RaTL and both anterior and posterior nodes of the OFC, which are associated with appraisal functions, as well as between the left basolateral amygdala and OFC. These results shed light on the importance of the RaTL and its functional connectivity with the OFC in accessing the hedonic evaluations required for accurate emotion identification, further supporting a hub-and-spoke model of socioemotional semantic processing for emotions (Binney and Ramsey, 2020; Lambon Ralph, 2014).

While this study used an uncommon study design, correlating trait functional connectivity with task performance outside of the scanner, there are multiple lines of support for the premise that behavior can be predicted by individual differences in trait ICN connectivity. Studies in healthy neurotypical individuals and in patients with neurodegeneration have shown that resting state connectivity predicts trait anxiety (Uddin, 2015), trait socioemotional sensitivity (Toller et al., 2018), interpersonal warmth (Toller et al., 2019), and executive test performance (Seeley et al., 2012). To check the validity of our approach, we conducted proof-of-principle analyses with control tasks and control networks to confirm that the relationship between SAN and emotion naming is specific, rather than a reflection of generalized loss of brain function or cognitive deficits, an error-checking approach that has been modeled elsewhere (Toller et al., 2018).

4.1. The semantic appraisal network and emotion reading

We found that stronger mean intrinsic connectivity in the SAN was associated with better emotion identification, extending previous studies showing an association between temporal lobe regional connectivity and emotion reading (Ranasinghe et al., 2016a). The direct association in our data between emotion identification and the connectivity between the RaTL and the orbitofrontal cortex suggests that identifying an emotion taps into both the domain-general semantic and the evaluative processes mediated by these SAN regions. This reflects what might be predicted based on the nature of the emotion identification task used in this study. Specifically, to correctly label another's emotional expression of (for example) 'disgust', one must retrieve multimodal semantic knowledge about disgust (facial expression, interoceptive experience, etc.), access a personalized hedonic evaluation of the stimulus (e.g., disgust is negatively valenced and evokes a sense of

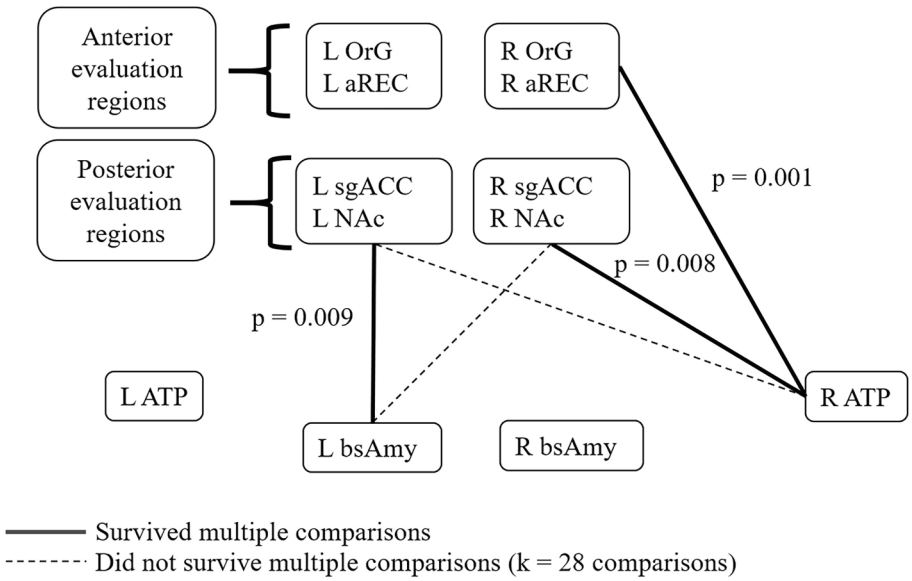

Fig. 3. shows the functional connectivity between nodes of the semantic appraisal network (SAN). Several regression models were conducted to investigate the functional connectivity between node-pairs of the SAN, after controlling for age, sex, and MMSE. A Benjamini-Yekutieli correction for k = 28 multiple comparisons was applied to the primary analysis, yielding a corrected significance threshold of $p < 0.01273$. We found that the functional connectivity between (1) the RaTP and the right posterior OFC evaluation node, (2) the RaTP and the right anterior OFC evaluation node, and (3) the left basolateral amygdala and the left posterior OFC evaluation node predicted TASIT-EET total score. All of these relationships remained significant after atrophy correction, and (1) and (2) remained significant in a rigorous error check for diagnostic confounding. OrG = orbital gyrus, aREC = anterior gyrus rectus, sgACC = subgenual anterior cingulate cortex, NAc = nucleus accumbens, aTP = anterior temporal pole, blAMY = basolateral amygdala, R = Right, L = Left.

aversion), and then compare these semantic-hedonic representations against the stimulus to more precisely determine if the emotion is disgust or another emotion (e.g. 'sadness').

These functional connections between the right-sided aTL semantic processing hub and orbitofrontal evaluation regions have previously been identified as important for facilitating the emotion identification process (Olson et al., 2013). The RaTL mediates learned conceptual knowledge about social behavior, while the OFC evaluation regions provide hedonic appraisal of the stimuli. These two regions, along with the amygdala, are bidirectionally anatomically connected via the uncinate fasciculus white matter tract (Ghashghaei and Barbas, 2002). The predominantly right-sided nature our results is consistent with evidence from a recent meta-analysis of functional neuroimaging studies, which argued that representation of semantics is supported by bilateral yet graded connectivity of the aTL, whereby the RaTL receives more sensory input relevant to emotional experience than the left (Rice et al., 2015) and thus may be comparatively more active in processing emotional semantics.

The anterior (rostral) and posterior (caudal) regions of the medial OFC, while both generally associated with evaluation, are known to have distinct functions and connectivity patterns (Kringelbach and Rolls, 2004). The posterior OFC (including the ventral striatum) is involved in reward anticipation, specifically related to its function in mapping discrepancy between predicted and actual reward values (O'Doherty et al., 2004). The nucleus accumbens encodes reward anticipation (Diekhof et al., 2012) and aids in resolving ambiguity around reward expectancy (Báez-Mendoza and Schultz, 2013). While this posterior OFC represents the reward value of primary reinforcers such as taste and visceral emotions (e.g. pain), in contrast more abstract or complex reinforcers such as monetary gain or loss are represented in the anterior OFC regions (Kringelbach and Rolls, 2004). There is evidence that the rostromedial PFC mediates reward consumption by reflecting changes in reward value based on complex cues such as emotion and identity (Goodkind et al., 2012).

We found that connectivity between the RaTL and both anterior and posterior OFC evaluation regions were separately able to predict accuracy of emotion labeling. Based on the known structural connections in these regions (Papinutto et al., 2016) and interpreting the FC patterns seen in this study (Fig. 3), one hypothesis about the flow of information during emotion reading emerges. Potentially, the RaTL combines sensory information about an emotional stimulus into a semantic representation (e.g., "Emotion X"), then the posterior OFC evaluation region assesses the reward and punishment valence of Emotion X ("aversive"), and resolves any remaining ambiguity about the semantic identity of the stimulus based on that viscerally experienced valence ("this is disgust, not amusement"). Once the semantic nature of the stimulus is thus clarified, the RaTL may then relay the resulting more clearly identified semantic representation to the anterior OFC region, where more contextually nuanced and abstract hedonic evaluations of the emotion and potentially its consequences may occur. Our data show that reduced intrinsic connectivity between the RaTL and either OFC node reduces the accuracy of emotion reading, thus a breakdown at any stage of this hypothetical processing sequence may have behavioral consequences.

4.2. *Role of the amygdala connections to the SAN in emotion reading*

The basolateral amygdala has been widely associated with perception of emotion (Bickart et al., 2014); however, its role appears to be more specifically to alert the individual to salient stimuli, including those of emotional importance, such as potential social reward or punishment (Rademacher et al., 2010). In our study, greater connectivity between the left basolateral amygdala and the left posterior OFC evaluation regions predicted more accurate emotion identification. Consistent with our finding, altered connectivity between the basolateral amygdala and subgenual ACC has previously been related to inefficient appraisal and regulation of emotions in depressed children (Murphy et al., 2016). Mechanistically, when the basolateral amygdala alerts an individual to a stimulus, it evokes the nucleus accumbens to encode the reward value of that stimulus (Ambroggi et al., 2009). Enhanced firing of nucleus accumbens neurons in turn promotes reward-seeking behavior. The activation of this alerting-appraisal circuit may be relevant to emotion reading in settings where another's emotional expression has the potential to convey social reward or punishment and thus requires enhanced attention for accurate decoding.

We did not find that connectivity between the basolateral amygdala and the aTL predicted accuracy of emotion labeling, despite the fact that these regions are linked structurally (Bickart et al., 2014). This may indicate that the alerting function of the BA and the semantic function of the RaTL do not require tight coordination for accurate emotion naming. This result could also be specific to the emotion labeling task used in our study, because it was comparatively easy and did not require rapid or subtle emotional cue detection. It is possible that a more nuanced task with shorter temporal presentation would require tighter RaTL-basolateral amygdala connectivity to achieve accurate emotion reading.

4.3. The salience network: Attention to but not evaluation of emotion

While many studies of patients with socio-emotional deficits implicate the SN (e.g., bvFTD (Seeley et al., 2007a), autism (Green et al., 2016)), we found that SAN connectivity independently predicted emotion identification while SN connectivity did not. The SN is fundamental in salience-driven attention, thus is likely important for tonic social alertness, and connectivity in this network directly predicts individual variation in socioemotional sensitivity (Toller et al., 2018). While general social attentiveness may improve the likelihood of emotion detection and accurate emotion reading during real-life social interactions, in our study it was not observed to exert a strong independent influence on performance of a lab-based emotion identification task, even in patients with below-normal mean SN connectivity. This may have been because the focused nature of the test limited and directed patients' attention adequately enough that they could then perform downstream emotion processing. Our evidence instead highlighted the important role of the SAN in emotion identification once attention is secured, i.e. accessing social semantic and visceral hedonic information to accurately characterize the emotion after it has been noticed. Future testing with more realistically fast or subtle emotional stimuli might reveal a more important role of SN connectivity, or perhaps a meaningful interaction between SN and SAN network connectivity, in support of emotion labeling accuracy in real-life settings.

4.4. Clinical relevance for patients with neurodegeneration

Our finding that weaker connectivity in the SAN predicts less accurate emotion identification reveals an important mechanism for the emotion naming deficits seen in many patients. Patients with conditions leading to tonic disruption in the SAN may have trouble retrieving and evaluating emotional concepts, which may lead to loss of precision distinguishing among similar emotions when interpreting real-life emotional displays. Our study and others have found that some patients have difficulty reading emotions even at the very early stages of neurodegeneration (Nelis et al., 2011). While we found wide performance variability across individual patients, the average patient with either bvFTD or svPPA syndrome scored significantly worse than controls on the fairly simple multimodal emotion identification task in our study. However, our data further clarify that these deficits likely result from reduction of functional connectivity between the RaTL and other nodes of the SAN, and particularly a disconnection between the RaTL and orbitofrontal regions responsible for making evaluations. Though bvFTD patients are often presumed to have predominantly SN dysfunction, many also present with concurrent and even focal SAN involvement (Ranasinghe et al., 2016b) and bvFTD patients with volumetric changes to the SAN are more likely than other bvFTD patients to show emotion naming deficits (Ranasinghe et al., 2016a). Structural damage in regions associated with the SAN is the predominant characteristic of svPPA syndrome (Seeley et al., 2009), and though a majority of early svPPA patients have left greater than right hemisphere damage, they all develop right temporal involvement as the disease progresses (Seeley et al., 2005). Our data suggest that as svPPA patients lose intrinsic connectivity between the RaTL and OFC, this brain change is likely to be revealed in increasing clinical deficits in emotion discrimination (Hutchings et al., 2017).

5. Limitations and conclusions

Because our primary goal of was to demonstrate the relationship between ICN connectivity and emotion reading accuracy, this study was designed to maximize patient heterogeneity to discover this linear brain-behavior relationship, and thus does not focus on or clarify the cognitive or neural characteristics of any single patient group. This limits our ability to extrapolate to clinical applications, or to characterize syndrome-specific relationships between SAN function and emotion reading. Thus, a number of outstanding questions remain for future studies, including an examination of how emotion reading relates mechanistically to other cognitive functioning in the various neurodegenerative syndromes. Performance on lab-based emotion reading tests may be mediated in part by various non-emotional cognitive factors such as attention and memory (Miller et al., 2012), as well as non-emotional semantics (Bertoux et al., 2020). Thus, our cognitively impaired patients with neurodegeneration may have made errors in part due to non-social cognitive deficits. We included only patients who were very early in their disease course, at either a pre-dementia or very mild dementia stage, excluded cases where a trained clinician determined that the patient did not fully understand or attend to the test, and covaried MMSE score in our analyses as a proxy of overall cognition, steps which likely mitigated the impact of non-social cognitive deficits on our results. If emotion-reading performance was indeed significantly influenced by non-social cognitive deficits in our sample, it would have added more "noise" to weaken, rather than artificially enhance, our main brain-behavior finding in the SAN, thus the fact that our result was significant suggests a fairly robust signal. Additionally, studies are needed to comprehensively characterize the other cognitive contributions of the SAN, and to understand how these relate to emotion reading deficits. In particular, it will be valuable to identify more precisely the natural history of SAN dysfunction in these syndromes, determining how early in the disease course patients develop alterations in connectivity, and clarifying the relationship between these ICN changes and socio-emotional symptoms, including emotion reading deficits. Future studies should expand on investigation into svPPA patients in particular, as the SAN is selectively vulnerable early in that subgroup; enrolling genetically at-risk family members at the pre-symptomatic or very early symptomatic stage and following them longitudinally would address many of these outstanding questions. Finally, while we did not find a statistically significant interaction between SAN and SN connectivity to predict emotion identification, it showed a suggestive trend, indicating the interaction between the two networks may be meaningfully related to emotion reading in a larger sample. Further characterization of the interplay between SN and SAN in socioemotional functioning is needed.

These secondary considerations did not, however, weaken the main finding that individual differences in the degree of intrinsic network connectivity in a brain network responsible for semantics and individualized hedonic evaluation can predict accuracy of emotion identification. We found a wide degree of individual variability in FC in all four ICNs both within and between diagnostic groups, even in controls, suggesting ICN variability is not simply a result of a specific disease process. Our study suggests that older adults who begin to develop new-onset difficulties with identifying others' emotions may be losing intrinsic functional connectivity in the SAN, and that in some cases this may be an early symptom of neurodegeneration. Emotion reading tests such as the TASIT-EET should regularly be included in clinical neuropsychological testing batteries designed to identify individuals at risk for neurodegenerative disease.

CRediT authorship contribution statement

Winson F.Z. Yang: Conceptualization, Methodology, Software, Formal analysis, Visualization, Writing - original draft. **Gianina Toller:** Methodology, Software, Investigation, Formal analysis, Writing - review & editing. **Suzanne Shdo:** Methodology, Investigation, Writing - review & editing. **Sonja A. Kotz:** Supervision, Writing - review & editing. **Jesse Brown:** Methodology, Software, Writing - review & editing. **William W. Seeley:** Methodology, Writing - review & editing. **Joel H. Kramer:** Funding acquisition, Resources, Writing - review & editing. **Bruce L. Miller:** Funding acquisition, Resources, Writing - review & editing. **Katherine P. Rankin:** Conceptualization, Methodology, Investigation, Formal analysis, Funding acquisition, Resources, Writing - original draft.

Declaration of Competing Interest

The authors declare that they have no known competing financial interests or personal relationships that could have appeared to influence the work reported in this paper.

Acknowledgements

We thank the patients and their caregivers for participating in this research. This work was supported by the National Institutes of Health under Grant numbers R01AG029577 (PI: Rankin), K23-AG021606 (PI: Rankin), P01AG019724 (PI: Miller), P50AG023501 (PI: Miller); Larry L. Hillblom Foundation under Grant number 2002/2j (PI: Rankin), 2014-A-004-NET (PI: Kramer).

References

Ambroggi, F., Ishikawa, A., Fields, H.L., Nicola, S.M., 2009. Basolateral amygdala neurons facilitate reward-seeking behaviour by exciting nucelus accumbens neurons. Neuron 59, 648–661.
Andrews-Hanna, J.R., Reidler, J.S., Sepulcre, J., Poulin, R., Buckner, R.L., 2010. Functional-anatomic fractionation of the brain's default network. Neuron 65, 550–562.
Andrews-Hanna, J.R., Smallwood, J., Spreng, R.N., 2014. The default network and self-generated thought: component processes, dynamic control, and clinical relevance. Ann. N. Y. Acad. Sci. 1316, 29–52.
Ashburner, J., Barnes, G., Chen, C.-C., Daunizeau, J., Flandin, G., Friston, K., Jafarian, A., Kiebel, S., Kilner, J., Litvak, V., Moran, R., Penny, W., Razi, A., Stephan, K., Tak, S., Zeidman, P., Gitelman, D., Henson, R., Hutton, C., Glauche, V., Mattout, J., Phillips, C., 2020. SPM12 Manual.
Báez-Mendoza, R., Schultz, W., 2013. The role of the striatum in social behavior. Front. Neurosci. 7, 1–14.
Baez, S., Morales, J.P., Slachevsky, A., Torralva, T., Matus, C., Manes, F., Ibanez, A., 2016. Orbitofrontal and limbic signatures of empathic concern and intentional harm in the behavioral variant frontotemporal dementia. Cortex 75, 20–32.
Battistella, G., Henry, M., Gesierich, B., Wilson, S.M., Borghesani, V., Shwe, W., Miller, Z., Deleon, J., Miller, B.L., Jovicich, J., Papinutto, N., Dronkers, N.F., Seeley, W.W., Mandelli, M.L., Gorno-Tempini, M.L., 2019. Differential intrinsic functional connectivity changes in semantic variant primary progressive aphasia. Neuroimage Clin. 22, 101797.
Beissner, F., Meissner, K., Bar, K.J., Napadow, V., 2013. The autonomic brain: an activation likelihood estimation meta-analysis for central processing of autonomic function. J. Neurosci. 33, 10503–10511.
Bertoux, M., Duclos, H., Caillaud, M., Segobin, S., Merck, C., de La Sayette, V., Belliard, S., Desgranges, B., Eustache, F., Laisney, M., 2020. When affect overlaps with concept: emotion recognition in semantic variant of primary progressive aphasia. Brain 143, 3850–3864.
Bickart, K.C., Dickerson, B.C., Barrett, L.F., 2014. The amygdala as a hub in brain networks that support social life. Neuropsychologia 63, 235–248.
Binder, J.R., Desai, R.H., Graves, W.W., Conant, L.L., 2009. Where is the semantic system? A critical review and meta-analysis of 120 functional neuroimaging studies. Cereb. Cortex 19, 2767–2796.
Binney, R.J., Ramsey, R., 2020. Social Semantics: the role of conceptual knowledge and cognitive control in a neurobiological model of the social brain. Neurosci. Biobehav. Rev. 112, 28–38.
Brett, M., Anton, J.-L., Valabregue, R., Poline, J.-B., 2002a. Region of interest analysis using an SPM toolbox. NeuroImage 16.
Brett, M., Johnsrude, I.S., Owen, A.M., 2002b. The problem of functional localization in the human brain. Nat. Rev. Neurosci. 3, 243–249.
Buckner, R.L., DiNicola, L.M., 2019. The brain's default network: updated anatomy, physiology and evolving insights. Nat. Rev. Neurosci. 20, 593–608.
Buckner, R.L., Krienen, F.M., Castellanos, A., Diaz, J.C., Yeo, B.T., 2011. The organization of the human cerebellum estimated by intrinsic functional connectivity. J. Neurophysiol. 106, 2322–2345.
Caminiti, S.P., Canessa, N., Cerami, C., Dodich, A., Crespi, C., Iannaccone, S., Marcone, A., Falini, A., Cappa, S.F., 2015. Affective mentalizing and brain activity at rest in the behavioral variant of frontotemporal dementia. Neuroimage Clin. 9, 484–497.
Choi, E.Y., Yeo, B.T., Buckner, R.L., 2012. The organization of the human striatum estimated by intrinsic functional connectivity. J. Neurophysiol. 108, 2242–2263.
Diekhof, E.K., Kaps, L., Falkai, P., Gruber, O., 2012. The role of the human ventral striatum and the medial orbitofrontal cortex in the representation of reward magnitude – an activation likelihood estimation meta-analysis of neuroimaging studies of passive reward expectancy and outcome processing. Neuropsychologia 50, 1252–1266.
Dosenbach, N.U.F., Fair, D.A., Miezin, F.M., Cohen, A.L., Wenger, K.K., Dosenbach, R.A. T., Fox, M.D., Snyder, A.Z., Vincent, J.L., Raichle, M.E., Schlaggar, B.L., Petersen, S. E., 2007. Distinct brain networks for adaptive and stable task control in humans. Proc. Natl. Acad. Sci. U. S. A. 104, 11073–11078.
Ghashghaei, H.T., Barbas, H., 2002. Pathways for emotion: Interactions of prefrontal and anterior temporal pathways in the amygdala of the rhesus monkey. Neuroscience 115, 1261–1279.
Goodkind, M.S., Sollberger, M., Gyurak, A., Rosen, H.J., Rankin, K.P., Miller, B., Levenson, R., 2012. Tracking emotional valence: The role of the orbitofrontal cortex. Hum. Brain Mapp. 33, 753–762.
Gorno-Tempini, M., Hillis, A., Weintraub, S., Kertesz, A., Mendez, M., Cappa, S., Ogar, J., Rohrer, J., Black, S., Boeve, B., Manes, F., Dronkers, N., Vandenberghe, R., Rascovsky, K., Patterson, K., Miller, B., Knopman, D., Hodges, J., Mesulam, M., Grossman, M., 2011. Classification of primary progressive aphasia and its variants. Neurology 76, 1006–1014.
Green, S.A., Hernandez, L., Bookheimer, S.Y., Dapretto, M., 2016. Salience Network Connectivity in Autism Is Related to Brain and Behavioral Markers of Sensory Overresponsivity. J. Am. Acad. Child Adolesc. Psychiatry 55 (618–626), e611.
Guo, C.C., Gorno-Tempini, M.L., Gesierich, B., Henry, M., Trujillo, A., Shany-Ur, T., Jovicich, J., Robinson, S.D., Kramer, J.H., Rankin, K.P., Miller, B.L., Seeley, W.W., 2013. Anterior temporal lobe degeneration produces widespread network-driven dysfunction. Brain 136, 2979–2991.
Hodges, J.R., Patterson, K., 2007. Semantic dementia: a unique clinicopathological syndrome. Lancet Neurol. 6, 1004–1014.
Humphreys, G.F., Hoffman, P., Visser, M., Binney, R.J., Lambon Ralph, M.A., 2015. Establishing task- and modality-dependent dissociations between the semantic and default mode networks. Proc. Natl. Acad. Sci. U. S. A. 112, 7857–7862.
Hutchings, R., Palermo, R., Piguet, O., Kumfor, F., 2017. Disrupted face processing in frontotemporal dementia: a review of the clinical and neuroanatomical evidence. Neuropsychol. Rev. 27, 18–30.
Kringelbach, M.L., Rolls, E.T., 2004. The functional neuroanatomy of the human orbitofrontal cortex: evidence from neuroimaging and neuropsychology. Prog. Neurobiol. 72, 341–372.
Kumfor, F., Ibanez, A., Hutchings, R., Hazelton, J.L., Hodges, J.R., Piguet, O., 2018. Beyond the face: how context modulates emotion processing in frontotemporal dementia subtypes. Brain 141, 1172–1185.
Laird, A.R., Fox, P.M., Eickhoff, S.B., Turner, J.A., Ray, K.L., McKay, D.R., Glahn, D.C., Beckmann, C.F., Smith, S.M., Fox, P.T., 2011. Behavioral interpretations of intrinsic connectivity networks. J. Cognit. Neurosci. 23, 4022–4037.
Lambon Ralph, M.A., 2014. Neurocognitive insights on conceptual knowledge and its breakdown. Philos. Trans. R. Soc. B: Biol. Sci. 369, 20120392.
Lambon Ralph, M.A., Jefferies, E., Patterson, K., Rogers, T.T., 2017. The neural and computational bases of semantic cognition. Nat. Rev. Neurosci. 18, 42–55.
Litvan, I., Agid, Y., Jankovic, J., Goetz, C., Brandel, J.P., Lai, E.G., Wenning, G., D'Olhaberriague, L., Verny, M., Chaudhuri, K.R., McKee, A., Jellinger, K., Bartko, J. J., Mangone, C.A., Pearce, R.K.B., 1996. Accuracy of clinical criteria for the diagnosis of progressive supranuclear palsy (Steele-Richardson-Olszewski syndrome). Neurology 46, 922–930.
Lowe, M.J., Mock, B.J., Sorenson, J.A., 1998. Functional connectivity in single and multislice echoplanar imaging using resting-state fluctuations. NeuroImage 7, 119–132.
Marshall, C.R., Hardy, C.J.D., Russell, L.L., Bond, R.L., Sivasathiaseelan, H., Greaves, C., Moore, K.M., Agustus, J.L., van Leeuwen, J.E.P., Wastling, S.J., Rohrer, J.D., Kilner, J.M., Warren, J.D., 2019. The functional neuroanatomy of emotion processing in frontotemporal dementias. Brain 142, 2873–2887.
McDonald, S., Flanagan, S., Martin, I., Saunders, C., 2004. The ecological validity of TASIT: a test of social perception. Neuropsychol. Rehabil. 14, 285–302.
McKhann, G., Knopman, D.S., Chertkow, H., Hymann, B., Jack, C.R., Kawas, C., Klunk, W., Koroshetz, W., Manly, J., Mayeux, R., Mohs, R., Morris, J., Rossor, M., Scheltens, P., Carrillo, M., Weintrub, S., Phelphs, C., 2011. The diagnosis of dementia due to Alzheimer's disease: recommendations from the National Institute on Aging-Alzheimer's Association workgroups on diagnostic guidelines for Alzheimer's disease. Alzheimers Dementia 7, 263–269.
Miller, L.A., Hsieh, S., Lah, S., Savage, S., Hodges, J.R., Piguet, O., 2012. One size does not fit all: Face emotion processing impairments in semantic dementia, behavioural-variant frontotemporal dementia and Alzheimer's disease are mediated by distinct cognitive deficits. Behav. Neurol. 25, 53–60.
Mitchell, J.P., 2009. Inferences about mental states. Philos. Trans. R. Soc. London Ser. B, Biol. Sci. 364, 1309–1316.
Multani, N., Galantucci, S., Wilson, S.M., Shany-Ur, T., Poorzand, P., Growdon, M.E., Jang, J.Y., Kramer, J.H., Miller, B.L., Rankin, K.P., Gorno-Tempini, M.L., Tartaglia, M.C., 2017. Emotion detection deficits and changes in personality traits linked to loss of white matter integrity in primary progressive aphasia. Neuroimage Clin. 16, 447–454.
Murphy, E.R., Barch, D.M., Pagliaccio, D., Luby, J.L., Belden, A.C., 2016. Functional connectivity of the amygdala and subgenual cingulate during cognitive reappraisal of emotions in children with MDD history is associated with rumination. Dev. Cogn. Neurosci. 18, 86–100.
Nelis, S.M., Clare, L., Martyr, A., Markova, I., Roth, I., Woods, R.T., Whitaker, C.J., Morris, R.G., 2011. Awareness of social and emotional functioning in people with early-stage dementia and implications for carers. Aging Mental Health 15, 961–969.
Nickerson, L.D., 2018. Replication of Resting state-task network correspondence and novel findings on brain network activation during task fMRI in the human connectome project study. Sci. Rep. 8, 17543.
O'Doherty, J., Dayan, P., Schultz, J., Deichmann, R., Friston, K., Dolan, R.J., 2004. Dissociable role of ventral and dorsal striatum in instrumental conditioning. Science 304, 452–454.
Olson, I.R., McCoy, D., Klobusicky, E., Ross, L.A., 2013. Social cognition and the anterior temporal lobes: a review and theoretical framework. Soc. Cogn. Affective Neurosci. 8, 123–133.

Papinutto, N., Galantucci, S., Mandelli, M.L., Gesierich, B., Jovicich, J., Caverzasi, E., Henry, R.G., Seeley, W.W., Miller, B.L., Shapiro, K.A., Gorno-Tempini, M.L., 2016. Structural connectivity of the human anterior temporal lobe: a diffusion magnetic resonance imaging study. Hum. Brain Mapp. 37, 2210–2222.

Patterson, K., Nestor, P.J., Rogers, T.T., 2007. Where do you know what you know? The representation of semantic knowledge in the human brain. Nat. Rev. Neurosci. 8, 976–987.

Pobric, G., Lambon Ralph, M.A., Zahn, R., 2016. Hemispheric specialization within the superior anterior temporal cortex for social and nonsocial concepts. J. Cogn. Neurosci. 28, 351–360.

Possin, K.L., Laluz, V.R., Alcantar, O.Z., Miller, B.L., Kramer, J.H., 2011. Distinct neuroanatomical substrates and cognitive mechanisms of figure copy performance in Alzheimer's disease and behavioral variant frontotemporal dementia. Neuropsychologia 49, 43–48.

Power, J.D., Barnes, K.A., Snyder, A.Z., Schlaggar, B.L., Petersen, S.E., 2012. Spurious but systematic correlations in functional connectivity MRI networks arise from subject motion. NeuroImage 59, 2142–2154.

Rademacher, L., Krach, S., Kohls, G., Irmak, A., Gründer, G., Spreckelmeyer, K.N., 2010. Dissociation of neural networks for anticipation and consumption of monetary and social rewards. NeuroImage 49, 3276–3285.

Ranasinghe, K.G., Rankin, K.P., Lobach, I.V., Kramer, J.H., Sturm, V.E., Bettcher, B.M., Possin, K., You, S.C., Lamarre, A.K., Shany-Ur, T., Stephens, M.L., Perry, D.C., Lee, S. E., Miller, Z.A., Gorno-Tempini, M.L., Rosen, H.J., Boxer, A., Seeley, W.W., Rabinovici, G.D., Vossel, K.A., Miller, B.L., 2016a. Cognition and neuropsychiatry in behavioral variant frontotemporal dementia by disease stage. Neurology 86, 600–610.

Ranasinghe, K.G., Rankin, K.P., Pressman, P.S., Perry, D.C., Lobach, I.V., Seeley, W.W., Coppola, G., Karydas, A.M., Grinberg, L.T., Shany-Ur, T., Lee, S.E., Rabinovici, G.D., Rosen, H.J., Gorno-Tempini, M.L., Boxer, A.L., Miller, Z.A., Chiong, W., DeMay, M., Kramer, J.H., Possin, K.L., Sturm, V.E., Bettcher, B.M., Neylan, M., Zackey, D.D., Nguyen, L.A., Ketelle, R., Block, N., Wu, T.Q., Dallich, A., Russek, N., Caplan, A., Geschwind, D.H., Vossel, K.A., Miller, B.L., 2016b. Distinct subtypes of behavioral variant frontotemporal dementia based on patterns of network degeneration. JAMA Neurol. 73, 1078–1088.

Rankin, K.P., 2020. Brain networks supporting social cognition in dementia. Curr. Behav. Neurosci. Rep. 7, 203–211.

Rankin, K.P., Salazar, A., Gorno-tempini, M.L., Sollberger, M., Wilson, S.M., Pavlic, D., Stanley, C.M., Glenn, S., Weiner, M.W., Miller, B.L., 2009. Detecting sarcasm from paralinguistic cues: anatomic and cognitive correlates in neurodegenerative disease. NeuroImage 47, 2005–2015.

Rascovsky, K., Hodges, J.R., Knopman, D., Mendez, M.F., Kramer, J.H., Neuhaus, J., van Swieten, J.C., Seelaar, H., Dopper, E.G., Onyike, C.U., Hillis, A.E., Josephs, K.A., Boeve, B.F., Kertesz, A., Seeley, W.W., Rankin, K.P., Johnson, J.K., Gorno-Tempini, M.L., Rosen, H., Prioleau-Latham, C.E., Lee, A., Kipps, C.M., Lillo, P., Piguet, O., Rohrer, J.D., Rossor, M.N., Warren, J.D., Fox, N.C., Galasko, D., Salmon, D.P., Black, S.E., Mesulam, M., Weintraub, S., Dickerson, B.C., Diehl-Schmid, J., Pasquier, F., Deramecourt, V., Lebert, F., Pijnenburg, Y., Chow, T.W., Manes, F., Grafman, J., Cappa, S.F., Freedman, M., Grossman, M., Miller, B.L., 2011. Sensitivity of revised diagnostic criteria for the behavioral variant of frontotemporal dementia. Brain 134, 2456–2477.

Rice, G.E., Lambon Ralph, M.A., Hoffman, P., 2015. The roles of left versus right anterior temporal lobes in conceptual knowledge: an ALE meta-analysis of 97 functional neuroimaging studies. Cereb. Cortex 25, 4374–4391.

Rijpma, M.G., Shdo, S.M., Shany-Ur, T., Toller, G., Kramer, J.H., Miller, B.L., Rankin, K. P., 2021. Salience driven attention is pivotal to understanding others' intentions. Cognit. Neuropsychol. 38, 88–106.

Seeley, W.W., 2019. The salience network: a neural system for perceiving and responding to homeostatic demands. J. Neurosci. 39, 9878–9882.

Seeley, W.W., Bauer, A.M., Miller, B.L., Gorno-Tempini, M.L., Kramer, J.H., Weiner, M., Rosen, H.J., 2005. The natural history of temporal variant frontotemporal dementia. Neurology 64, 1384–1390.

Seeley, W.W., Crawford, R.K., Zhou, J., Miller, B.L., Greicius, M.D., 2009. Neurodegenerative diseases target large-scale human brain networks. Neuron 62, 42–52.

Seeley, W.W., Menon, V., Schatzberg, A.F., Keller, J., Glover, G.H., Kenna, H., Reiss, A.L., Greicius, M.D., 2007. Dissociable intrinsic connectivity networks for salience processing and executive control. J. Neurosci. 27, 2349–2356.

Seeley, W.W., Zhou, J., Kim, E.-J., 2012. Frontotemporal dementia: What can the behavioral variant teach us about human brain organization? The Neuroscientist 18, 373–385.

Smith, S.M., Fox, P.T., Miller, K.L., Glahn, D.C., Fox, P.M., Mackay, C.E., Filippini, N., Watkins, K.E., Toro, R., Laird, A.R., Beckmann, C.F., 2009. Correspondence of the brain's functional architecture during activation and rest. Proc. Natl. Acad. Sci. 106, 13040–13045.

Sollberger, M., Stanley, C.M., Wilson, S.M., Gyurak, A., Beckman, V., Growdon, M., Jang, J., Weiner, M.W., Miller, B.L., Rankin, K.P., 2009. Neural basis of interpersonal traits in neurodegenerative diseases. Neuropsychologia 47, 2812–2827.

Stein, J.L., Wiedholz, L.M., Bassett, D.S., Weinberger, D.R., Zink, C.F., Mattay, V.S., Meyer-Lindenberg, A., 2007. A validated network of effective amygdala connectivity. NeuroImage 36, 736–745.

Toller, G., Brown, J., Sollberger, M., Shdo, S., Bouvet, L., Sukhanov, P., Seeley, W.W., Miller, B.L., Rankin, K.P., 2018. Individual differences in socioemotional sensitivity are an index of salience network function. Cortex.

Toller, G., Yang, W.F.Z., Brown, J.A., Ranasinghe, K.G., Shdo, S.M., Kramer, J.H., Seeley, W.W., Miller, B.L., Rankin, K.P., 2019. Divergent patterns of loss of interpersonal warmth in frontotemporal dementia syndromes are predicted by altered intrinsic network connectivity. Neuroimage Clin. 22, 101729.

Uddin, L.Q., 2015. Salience processing and insular cortical function and dysfunction. Nat. Rev. Neurosci. 16, 55–61.

Van den Stock, J., Stam, D., De Winter, F.L., Mantini, D., Szmrecsanyi, B., Van Laere, K., Vandenberghe, R., Vandenbulcke, M., 2017. Moral processing deficit in behavioral variant frontotemporal dementia is associated with facial emotion recognition and brain changes in default mode and salience network areas. Brain Behav. 7, e00843.

Van Dijk, K.R.A., Sabuncu, M.R., Buckner, R.L., 2012. The influence of head motion on intrinsic functional connectivity MRI. Neuroimage 59, 431–438.

Wang, X., Wang, B., Bi, Y., 2019. Close yet independent: dissociation of social from valence and abstract semantic dimensions in the left anterior temporal lobe. Hum. Brain Mapp. 40, 4759–4776.

Yeo, B.T., Krienen, F.M., Chee, M.W., Buckner, R.L., 2014. Estimates of segregation and overlap of functional connectivity networks in the human cerebral cortex. NeuroImage 88, 212–227.

Yeo, B.T.T., Krienen, F.M., Sepulcre, J., Sabuncu, M.R., Lashkari, D., Hollinshead, M., Roffman, J.L., Smoller, J.W., Zollei, L., Polimeni, J.R., Fischl, B., Liu, H., Buckner, R. L., 2011. The organization of the human cerebral cortex estimated by intrinsic functional connectivity. J. Neurophysiol. 106, 1125–1165.

Zhou, J., Greicius, M.D., Gennatas, E.D., Growdon, M.E., Jang, J.Y., Rabinovici, G.D., Kramer, J.H., Weiner, M., Miller, B.L., Seeley, W.W., 2010. Divergent network connectivity changes in behavioural variant frontotemporal dementia and Alzheimer's disease. Brain 133, 1352–1367.

Zielinski, B.A., Gennatas, E.D., Zhou, J., Seeley, W.W., 2010. Network-level structural covariance in the developing brain. Proc. Natl. Acad. Sci. 107, 18191–18196.